AGU100 ADVANCING EARTH AND SPACE SCIENCE

JGR

Journal of Geophysical Research: Atmospheres

RESEARCH ARTICLE

10.1002/2017JD027943

Key Points:

- The impacts of different ozone representations in climate sensitivity simulations are assessed with HadGEM3-AO
- We find significant impacts on global warming and other composition-climate feedbacks, such as the stratospheric water vapor feedback
- Our results imply that some ozone implementations in climate sensitivity simulations need to be reconsidered

Correspondence to:
P. J. Nowack,
p.nowack@imperial.ac.uk

Citation:
Nowack, P. J., Abraham, N. L., Braesicke, P., & Pyle, J. A. (2018). The impact of stratospheric ozone feedbacks on climate sensitivity estimates. *Journal of Geophysical Research: Atmospheres*, *123*, 4630–4641. https://doi.org/10.1002/2017JD027943

Received 1 DEC 2017
Accepted 1 MAR 2018
Accepted article online 18 APR 2018
Published online 2 MAY 2018

The Impact of Stratospheric Ozone Feedbacks on Climate Sensitivity Estimates

Peer J. Nowack[1,2], N. Luke Abraham[1,3], Peter Braesicke[4], and John A. Pyle[1,3]

[1]Department of Chemistry, Centre for Atmospheric Science, University of Cambridge, Cambridge, UK, [2]Now at Grantham Institute, Department of Physics and the Data Science Institute, Faculty of Natural Sciences, Imperial College London, London, UK, [3]National Centre for Atmospheric Science, UK, [4]Karlsruhe Institute of Technology, IMK-ASF, Karlsruhe, Germany

Abstract A number of climate modeling studies have shown that differences between typical choices for representing ozone can affect climate change projections. Here we investigate potential climate impacts of a specific ozone representation used in simulations of the Hadley Centre Global Environment Model for the Coupled Model Intercomparison Project Phase 5. The method considers ozone changes only in the troposphere and lower stratosphere and prescribes stratospheric ozone elsewhere. For a standard climate sensitivity simulation, we find that this method leads to significantly increased global warming and specific patterns of regional surface warming compared with a fully interactive atmospheric chemistry setup. We explain this mainly by the suppressed part of the stratospheric ozone changes and the associated alteration of the stratospheric water vapor feedback. This combined effect is modulated by simultaneous cirrus cloud changes. We underline the need to understand better how representations of ozone can affect climate modeling results and, in particular, global and regional climate sensitivity estimates.

1. Introduction

Atmospheric ozone is a key absorber of solar radiation and an important greenhouse gas. Consequently, a large sensitivity of surface temperature to ozone changes has been evident for a long time, even in idealized radiative transfer calculations that did not consider many climate feedbacks (e.g., Lacis et al., 1990). This sensitivity is particularly distinct for ozone changes in the tropical upper troposphere and lower stratosphere (UTLS; see, e.g., Figure 1 in Riese et al., 2012). Here we explore how considering or (to some extent) neglecting ozone changes under climate change alters the climate sensitivity of a fully interactive atmosphere-ocean coupled climate model. Our work stands in context with a number of recent studies that have confirmed that the representation of ozone in state-of-the-art climate models can affect tropospheric and surface climate change projections (e.g., Chiodo & Polvani, 2016a, 2016b; Dietmüller et al., 2014; Muthers et al., 2014, 2016; Noda et al., 2017; Nowack et al., 2015, 2017; Son et al., 2008). It is further motivated by the apparently strong model and scenario dependency of climate impacts associated with changes in ozone. For example, current estimates for the impact of interactive ozone chemistry on global warming projections for a typical climate sensitivity simulation range between none (Marsh et al., 2016) and ~20% difference (Nowack et al., 2015).

Atmospheric chemistry (and thus ozone) has been represented in a variety of ways in climate models, in particular in model intercomparison projects (Cionni et al., 2011; Eyring et al., 2013; Kravitz et al., 2013; Son et al., 2008; Taylor et al., 2012). For example, only 9 of 46 climate models used to simulate the four Representative Concentration Pathways (RCP) scenarios in the Coupled Model Intercomparison Project Phase 5 (CMIP5) included a fully interactive chemistry scheme in both the troposphere and the stratosphere (Eyring et al., 2013). In acknowledgement of the importance of ozone, the chemistry-climate community therefore provided a standardized IGAC/SPARC ozone field for RCP simulations to be used in models without atmospheric chemistry component (Cionni et al., 2011). While this posed an improvement over neglecting ozone changes altogether in many similar CMIP3 simulations (Son et al., 2008), this ozone field was inconsistent with both the actual RCP scenarios and individual model responses. In contrast, there was no organized or unified effort concerning the representation of ozone in typical climate sensitivity simulations in CMIP5, such as those imposing an abrupt quadrupling of atmospheric carbon dioxide (CO_2). As a result, models that lacked the capability to simulate ozone changes on the run had to represent ozone inconsistently, for example, by neglecting ozone changes or by using other methods. While it is not well documented how ozone was treated in such cases (with a few exceptions, e.g., Jones et al., 2011; Li et al., 2013), it is highly likely that the

majority of models used unchanged climatologies, or some other form of noninteractive ozone fields in typical climate sensitivity experiments. Consequently, there is a need to understand better how climate sensitivity simulations have been shaped by the representation of ozone in conjunction with other parametric choices. It is almost self-evident that this need for an improved understanding of ozone's role in climate sensitivity simulations extends beyond the CMIP framework.

Here we investigate one example of potential effects on climate sensitivity projections for a specific ozone representation that was used by the UK Met Office in HadGEM2-ES simulations for the CMIP5 (Jones et al., 2011). Specifically, we test its effect on the outcome of a standard climate sensitivity simulation in which CO_2 concentrations are abruptly quadrupled. For this, we carry out the same analysis as in a previously published paper (Nowack et al., 2015), where we found that neglecting changes in ozone (also referred to as ozone feedbacks) leads to ~20% increased global warming for the same climate model and experiment.

In HadGEM2-ES, the implementation of this method included an interactive representation of tropospheric and lower stratospheric ozone; that is, ozone was allowed to respond to the CO_2 forcing in this lower part of the atmosphere. The ozone field was fixed elsewhere, meaning that ozone was not allowed to adapt in the middle-upper stratosphere. In the following, we focus on how this representation of ozone modulates global warming in our model. In addition, we show that it can explain stratospheric water vapor (SVW) results obtained in the corresponding CMIP5 simulation with HadGEM2-ES. Indirectly, this method allows us to test the importance of changes in ozone specifically in the lower part of the atmosphere including the tropical UTLS. At the same time, we explain why it may generally be deceptive to study ozone changes in certain regions in isolation, mainly because ozone concentrations in different parts of the atmosphere are intrinsically coupled.

The method used in HadGEM2-ES should pose an improvement on neglecting ozone changes altogether (as probably done in many climate sensitivity studies), but without detailed study, it is impossible to quantify this improvement. We further discuss our results in the context of recent studies on ozone-related effects in climate sensitivity experiments.

2. Methods

2.1. Model

We use the atmosphere-ocean coupled configuration of the Hadley Centre Global Environment Model version 3 (HadGEM3-AO) from the UK Met Office (Hewitt et al., 2011). The atmosphere is represented by the Met Office's Unified Model version 7.3 using a regular grid with a horizontal resolution of 3.75° longitude by 2.5° latitude and 60 vertical levels up to a height of ~84 km. The ocean component is the Ocean Parallélisé (OPA) part of the Nucleus for European Modelling of the Ocean (NEMO) model version 3.0 (Madec, 2008) coupled to the Los Alamos sea ice model CICE version 4.0 (Hunke & Lipscomb, 2008). The NEMO configuration used here deploys a tripolar, locally anisotropic grid which has 2° resolution in longitude everywhere, but an increased latitudinal resolution in certain regions with up to 0.5° in the tropics.

Atmospheric chemistry is represented by the UK Chemistry and Aerosols model in an updated version of the detailed stratospheric chemistry configuration (Morgenstern et al., 2009; Nowack et al., 2015, 2016, 2017), which is coupled to the Met Office's Unified Model. A relatively simple tropospheric chemistry scheme that simulates hydrocarbon oxidation is included, which provides for emissions of three chemical species (NO [surface and lightning], CO [surface], and HCHO [surface]). In addition, surface mixing ratios of four further species (N_2O, CH_3Br, H_2, and CH_4) are constrained by calculating the effective emission required to maintain their surface mixing ratios, for example, for nitrous oxide 280 ppbv and methane 790 ppbv. This keeps their tropospheric mixing ratios approximately constant at preindustrial levels in all simulations. Nitrogen oxide emissions from lightning are parameterized according to Price and Rind (1992, 1994). Photolysis rates are calculated interactively using the Fast-JX photolysis scheme (Bian & Prather, 2002; Neu et al., 2007; Telford et al., 2013; Wild et al., 2000). In total, 159 chemical reactions involving 41 chemical species are considered. The chemistry scheme used here is different from the one used for the corresponding HadGEM2-ES simulation in CMIP5, as discussed in section 2.2.

Table 1
Overview of the Simulations

	Label	Representation of ozone
piControl	A	Interactive in the whole atmosphere
$4xCO_2$	B	
$4xCO_2$	D1	Interactive in the troposphere and the lowermost three model levels of the stratosphere, prescribed climatology (zonally averaged for D2) from A above
$4xCO_2$	D2	

Note. Two versions (i.e., D1/D2) of the tropopause-matched runs were carried out. The label 1 implies that the chemical fields were overwritten from three model levels above the tropopause upward by full three-dimensional (latitude, longitude, and altitude) monthly mean climatologies from piControl run A. In D2, the same climatologies were zonally averaged and as such imposed as three-dimensional fields, with almost identical results.

2.2. Simulations

To study the impact of the model representation of ozone on climate sensitivity results, we first carried out a preindustrial control simulation (piControl, 285 ppmv CO_2, label A) and, second, typical climate sensitivity simulations in which atmospheric CO_2 was abruptly quadrupled to four times its preindustrial value (hereafter referred to as $4xCO_2$, 1,140 ppmv CO_2). Such simulations are standard experiments in model intercomparison projects (Eyring et al., 2016; Kravitz et al., 2013; Taylor et al., 2012). Each simulation was run for 200 years (for an overview see Table 1).

The $4xCO_2$ benchmark simulation with fully interactive chemistry is referred to as "B." In two further $4xCO_2$ simulations, which we here label D1 and D2 in order to conform with a previous paper (Nowack et al., 2017), we emulate the model setup described by Jones et al. (2011) for the abrupt $4xCO_2$ experiment carried out with the HadGEM2-ES model for the CMIP5. In D1 and D2, the distribution of the radiatively active species ozone, nitrous oxide, and methane was reset to preindustrial levels from three model levels above the continuously changing tropopause (Hoerling et al., 1993) upward. In other words, ozone was only allowed to change from the surface up to three model levels above the tropopause and was otherwise kept fixed in terms of its mass mixing ratio. The vertical distance between the tropopause and the overwritten stratospheric levels is between ~3 and 4 km at all latitudes. This specific methodology used in D1/D2 is referred to as "tropopause-matching" in the following.

The tropopause-matched model setup will necessarily include to some degree ozone feedbacks in the tropical UTLS, which were previously identified as a key driver of ozone's impact on climate sensitivity estimates (Dietmüller et al., 2014; Forster & Shine, 1997; Hansen et al., 1997; Lacis et al., 1990; Nowack et al., 2015). It will also prevent an artificial mismatch between ozone and the atmospheric pressure/temperature profiles around the tropopause. This is important due to the steep gradient in ozone mass mixing ratios between the upper troposphere and lower stratosphere; that is, it prevents high stratospheric ozone levels from being shifted into the troposphere when the latter expands under CO_2 forcing (Dietmüller et al., 2014; Heinemann, 2009; Li et al., 2013; Nowack et al., 2015).

The ozone methodology applied in D1/D2 is identical to the setup of the HadGEM2-ES model for the abrupt $4xCO_2$ simulation in CMIP5, and the atmosphere part of HadGEM2-ES is the predecessor model of the atmospheric component of the HadGEM3 model used here. Nevertheless, there are several key differences between our simulations and the HadGEM2-ES implementation. HadGEM2-ES is a low-top model that does not include a full representation of the stratosphere (reaching up to ~40-km altitude; Collins et al., 2011). In addition, HadGEM2-ES included a somewhat more sophisticated tropospheric chemistry scheme, but no specific stratospheric chemistry, in contrast to the scheme used here. It is impossible to estimate precisely how these and other differences in the model setup could affect, in relative terms, the results. However, our setup is sufficient to consider how this alternative representation of ozone feedbacks can affect climate sensitivity, forcing, and feedback estimates in a qualitative manner as compared to a fully interactive chemistry configuration.

2.3. Method to Estimate Climate Forcings and Feedbacks

In section 3.2, we apply the linear regression methodology suggested by Gregory et al. (2004) to diagnose global climate feedbacks and forcings. The method has been shown to capture well the response of models to many types of climate forcing (Gregory & Webb, 2008; Forster et al., 2016). It assumes a linear relationship between the change in global and annual mean radiative imbalance N (W/m^2) at the top of the atmosphere and surface temperature anomalies (ΔT_{surf}, in K) relative to a base climate state (typically preindustrial):

$$N = F + \alpha\, \Delta T_{surf} \tag{1}$$

where the y-intercept F is the effective forcing (W/m^2) and the slope α is the effective climate feedback parameter ($W \cdot m^{-2} \cdot K^{-1}$). Thus, α and F can be obtained by regressing N as a function of time against ΔT_{surf}. α is a characteristic quantity of a given model system, because its magnitude approximates the surface

temperature response to a radiative forcing introduced to the system. Here the positive sign convention is used, meaning that a negative α implies a stable climate system that will eventually attain equilibrium. Any positive/negative change in α implies an additional surface warming/cooling at equilibrium in response to a radiative forcing.

The Gregory method, and more generally energy budget considerations, are often extended by the assumption that the net climate feedback parameter α (and accordingly F) can be approximated by a linear superposition of processes that contribute to the overall climate response to an imposed forcing, that is

$$\alpha = \sum_i \alpha_i \tag{2.1}$$

$$F = \sum_i F_i \tag{2.2}$$

Accordingly, one can decompose α and F into separate radiative components (Andrews et al., 2012)

$$\alpha = \alpha_{CS} + \alpha_{CRE} = \alpha_{CS,LW+}\ \alpha_{CS,SW} + \alpha_{CRE,LW} + \alpha_{CRE,SW} \tag{3.1}$$

$$F = F_{CS} + F_{CRE} = F_{CS,LW+}\ F_{CS,SW} + F_{CRE,LW} + F_{CRE,SW} \tag{3.2}$$

providing individual shortwave (SW) and long-wave (LW) components for clear-sky (CS) radiative fluxes and the cloud radiative effect (CRE). The CS values refer to idealized radiative calculations in which any cloud effects are left out. The CRE component then represents the difference between the all-sky calculations including clouds and this CS component. In this method, the CRE contains direct effects due to changes in clouds and indirect cloud masking effects, for example, due to persistent cloud cover over certain areas of the globe that mask surface albedo changes in the all-sky calculation (Soden et al., 2004; Soden et al., 2008; Zelinka et al., 2013). The individual α and F components can be obtained by component-wise regressions of the radiative fluxes against ΔT_{surf}.

3. Results

3.1. Surface Warming Response

Figure 1a shows ΔT_{surf} for all runs relative to the average of piControl. Following a sharp increase after the abrupt 4xCO_2 forcing, surface temperatures for the tropopause-matched runs D1/D2 level off toward a higher equilibrium value than for fully interactive run B. Specifically, the global mean surface warming after 75 years is ~7% larger in D1/D2 than in B, which is about one third of the effect of neglecting ozone feedback entirely for the same model (Nowack et al., 2015). As expected, there is still a remaining temperature trend after 200 years in all 4xCO_2 runs due to the long oceanic timescales involved in attaining equilibrium (Knutti & Rugenstein, 2015; Li et al., 2013). Due to the different warming trajectories, the percentage difference decreases slightly over time, approaching ~6.5% toward the end of the 200-year runtime.

Regional surface temperatures also differ significantly between D1/D2 and B and have a specific regional structure (Figures 1b–1e). This implies that the stratospheric representation of ozone does not only alter the scaling of the surface temperature response to CO_2 forcing in a globally uniform manner but has a specific forcing-response pattern and alters regional feedbacks (Boer & Yu, 2003a, 2003b; Shindell & Faluvegi, 2009; Voulgarakis & Shindell, 2010). A detailed discussion of regional impacts is beyond the scope of this simple global energy budget paper. However, ozone-induced differences in the El Niño Southern Oscillation between the simulations (Nowack et al., 2017), associated changes in atmospheric teleconnections, or a modulating effect of ozone changes on the Atlantic Meridional Overturning Circulation (Muthers et al., 2016) could explain some of these regional responses. The pattern and magnitude of the surface temperature anomalies are mostly very similar for D1 and D2, implying that the surface impacts related to zonal averaging of the ozone climatology are small compared to the ones between B and D1/D2. The existing regional anomalies, for example, in the Barents Sea, could be related to the effects of the different zonal structure of the ozone fields used in D1 and D2 on the stratospheric temperature structure and dynamics (Gabriel et al., 2007) and by extension their possible tropospheric impacts. However, a proper analysis would have to take into account a number of other factors, including the state of the ocean and its interaction with sea ice feedback.

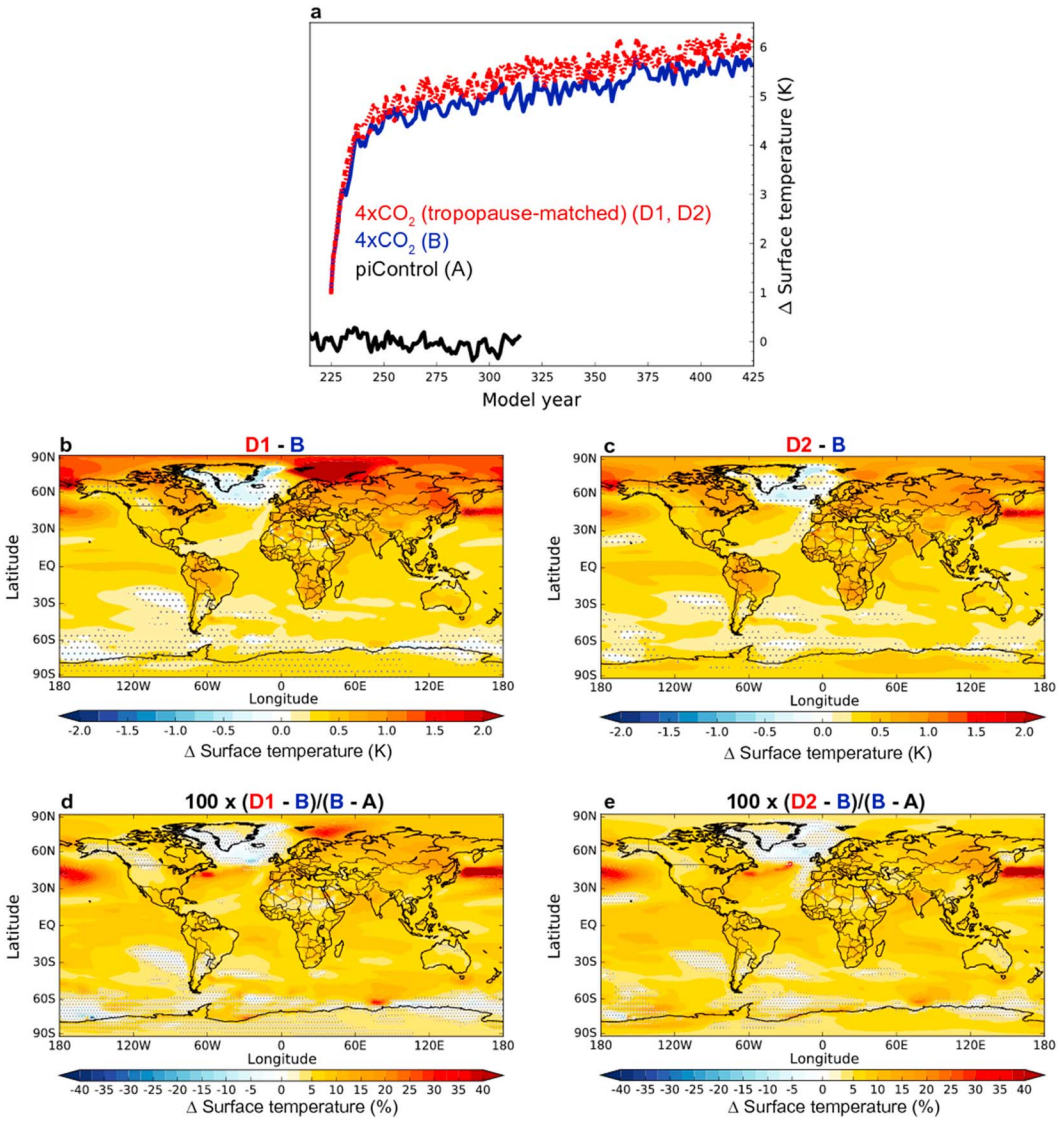

Figure 1. (a) Global, annual mean surface temperature anomalies. The time axis is extended to Figure 1 in Nowack et al. (2015). The red dashed/dotted lines denote runs D1/D2, respectively. (b and c) Regional differences as labeled, averaged over years 275–425 of (a), i.e., years 50–200 after the initialization of the $4xCO_2$ forcing. (d and e) The same regional differences given as percentage changes relative to the warming under $4xCO_2$ for B. The global mean difference is ~7%. Nonsignificant changes (95% confidence level, two-tailed Student's *t* test) are marked by stippling.

3.2. Global Energy Budget Analysis

To illustrate key differences between the simulations, we carried out the linear regression analysis as described in section 2.3. The results for the all-sky regression and the four individual CS and CRE components are given in Figures 2a–2e.

The α feedback parameters of B, D1, and D2 are almost identical (Figure 2a, inset table). The individual CS and CRE components reveal that this is primarily the result of two canceling factors: the $\alpha_{CS,LW}$ parameters in D1/D2 are less negative (by ~0.1 $W \cdot m^{-2} \cdot K^{-1}$; Figure 2b), thus indicating an additional surface warming effect in agreement with the results shown in Figure 1. However, this less negative feedback in D1/D2 is largely compensated by simultaneous, opposite sign $\alpha_{CRE,LW}$ changes (~0.07 $W \cdot m^{-2} \cdot K^{-1}$; Figure 2c). The additional surface warming in D1/D2 relative to B would be even more significant without this compensating CRE-LW feedback.

In comparison, changes in the SW components play a minor role (Figures 2d and 2e). Overall, this gives rise to the very similar, however, still slightly less negative total α parameters in D1/D2, consistent with the greater

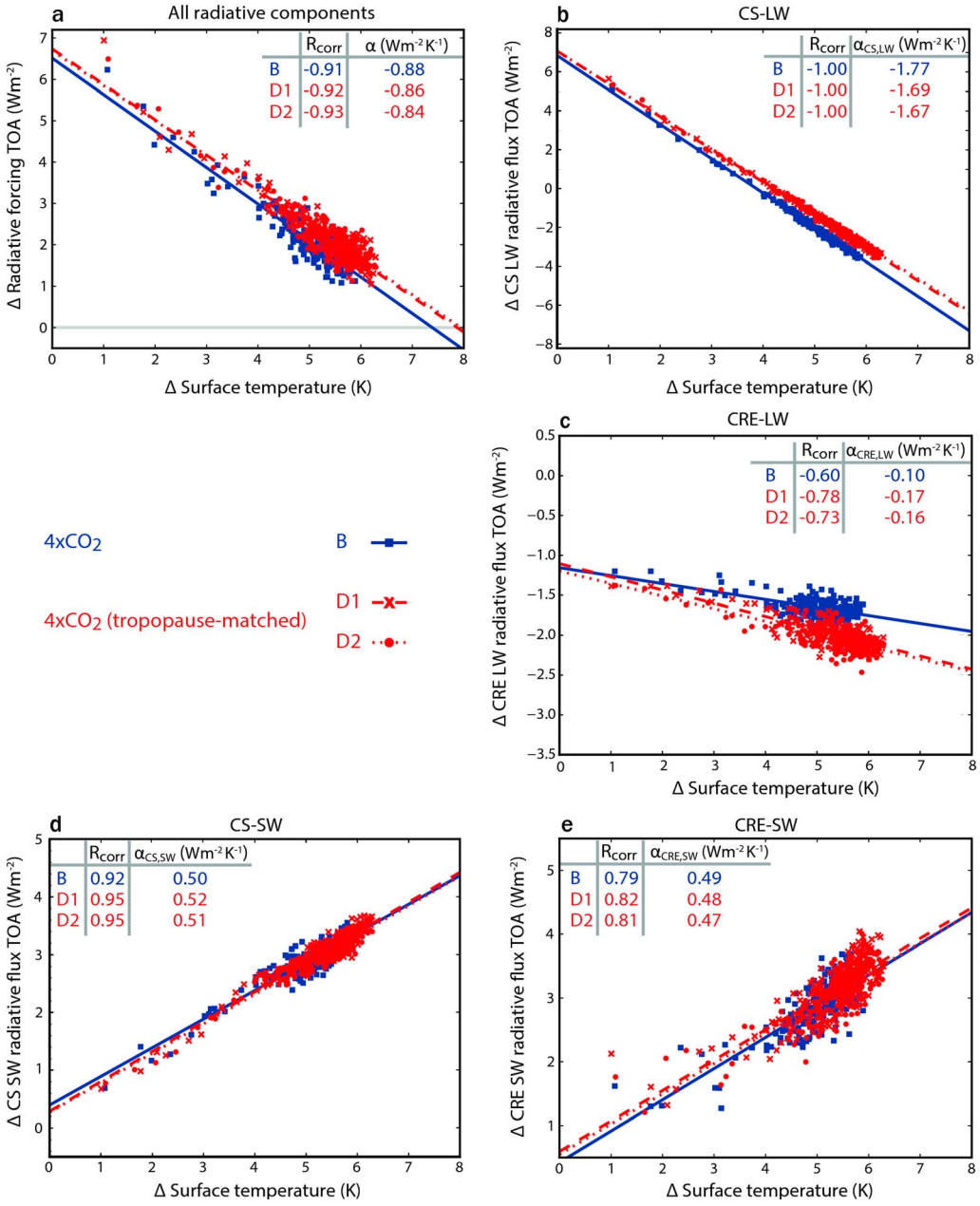

Figure 2. Gregory regressions for all 4xCO_2 simulations as labeled. For (a) the total net TOA radiative flux and (b)–(e) the four subcomponents. The inset tables give the slopes (i.e., the effective feedback parameters α) and regression coefficients (R_{corr}).

surface warming in these runs. This surplus warming is enhanced by ~0.2 W/m^2 more positive effective forcings *F* in D1/D2 (*y*-intercepts in Figure 2a). These characterize fast (and actually nonlinear; the data deviate from the regression lines toward $\Delta T_{surf} = 0$) adjustments in response to the CO_2 forcing (Forster et al., 2013; Sherwood et al., 2015; Zelinka et al., 2013).

3.3. The Mechanism

The differences in global warming between the simulations can mainly be understood from the representation of ozone and associated SVW and cirrus cloud feedback. This argument is equivalent to the mechanism described in Nowack et al. (2015), but the absolute and relative magnitude of each contribution differs. As a result, surface temperatures in D1/D2 are closer to B than if ozone feedbacks are neglected altogether (as done in our previous study).

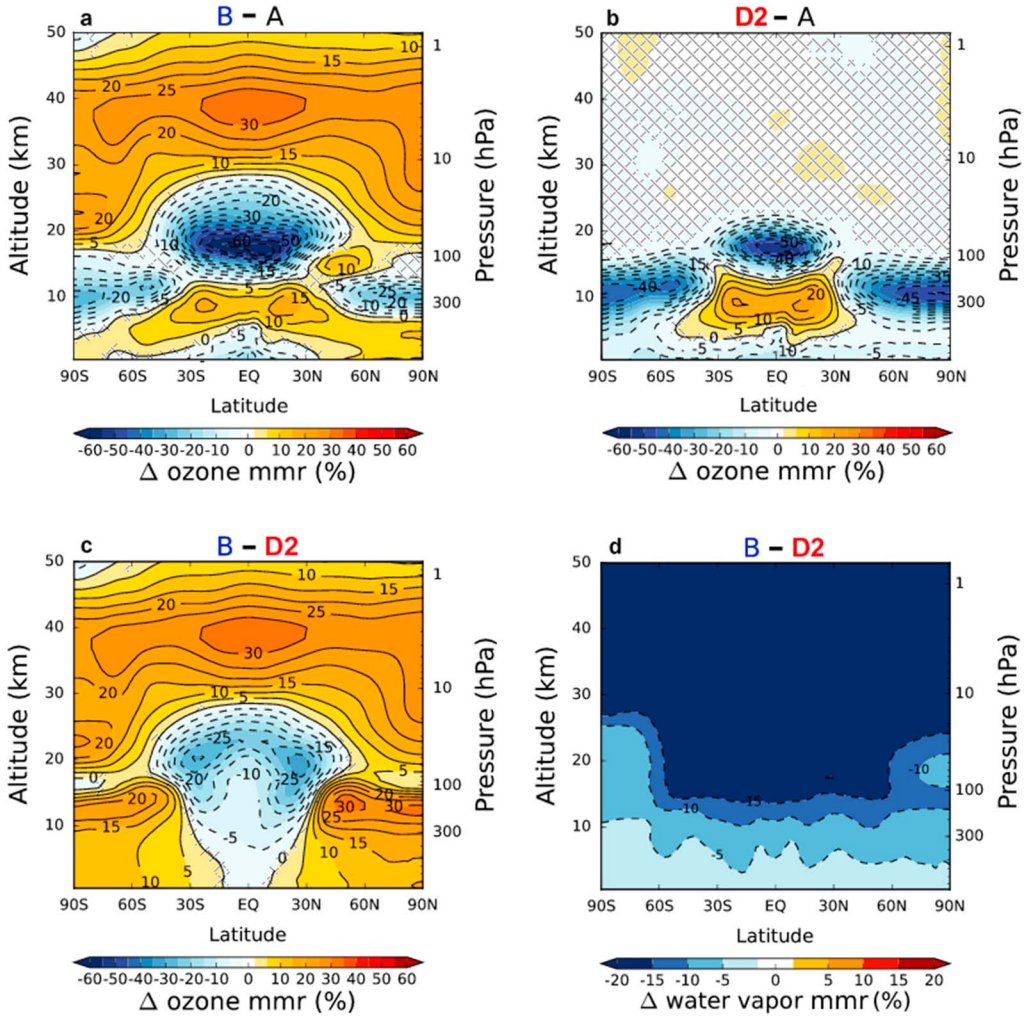

Figure 3. (a–d) Zonal mean ozone and water vapor percentage differences, as labeled, for years 50–200 after the 4xCO_2 forcing. Nonsignificant changes at the 95% confidence level using a two-tailed Student's *t* test are hatched out. Small artifacts at overwritten altitudes in (b) result from ozone changes between the dynamical and chemistry model time-steps, which occur before the ozone field is reset to preindustrial values. (c) The difference between (a) and (b).

Figures 3a and 3b show latitude-height cross sections of percentage changes in annual, zonal mean ozone mass mixing ratios under 4xCO_2 for both the fully interactive and the tropopause-matched runs (here discussed for D2, but with equivalent results for D1). We find characteristic decreases in tropical UTLS ozone within ~30°N–30°S. This is an ubiquitous feature in chemistry-climate model simulations under increased atmospheric greenhouse gas concentrations that has mainly been explained by an acceleration of the stratospheric Brewer-Dobson circulation (SPARC, 2010; Lin & Fu, 2013). Middle-upper stratospheric ozone increases found in the fully interactive run B under CO_2-induced cooling of the stratosphere are also well understood (Haigh & Pyle, 1982; Jonsson et al., 2004).

However, the tropopause-matching method fails to capture the full magnitude and spatial extent of the ozone decreases in the tropical UTLS (compare Figures 3a and 3b; for the actual difference between B and D2 see Figure 3c). The proximity to the fixed ozone boundary conditions above tends to level out the ozone decrease below by diffusion. More advective in-mixing of stratospheric ozone into the tropical UTLS via the shallow branch of the Brewer-Dobson circulation will support this effect. The larger mid-to-upper tropospheric ozone increases in D1/D2 than in B are likely the sum of elevated lightning NO_x emissions under greenhouse gas forcing and this is greater in-mixing of ozone. In addition, the lack of temperature-driven increases in upper stratospheric ozone in D1/D2 enhance ozone production in the tropical UTLS relative to B due to the reverse self-healing effect of the ozone column (Haigh & Pyle, 1982; Meul et al., 2014; Pyle, 1980); that is, changes in ozone formation at different altitudes are anticorrelated as increases in ozone at

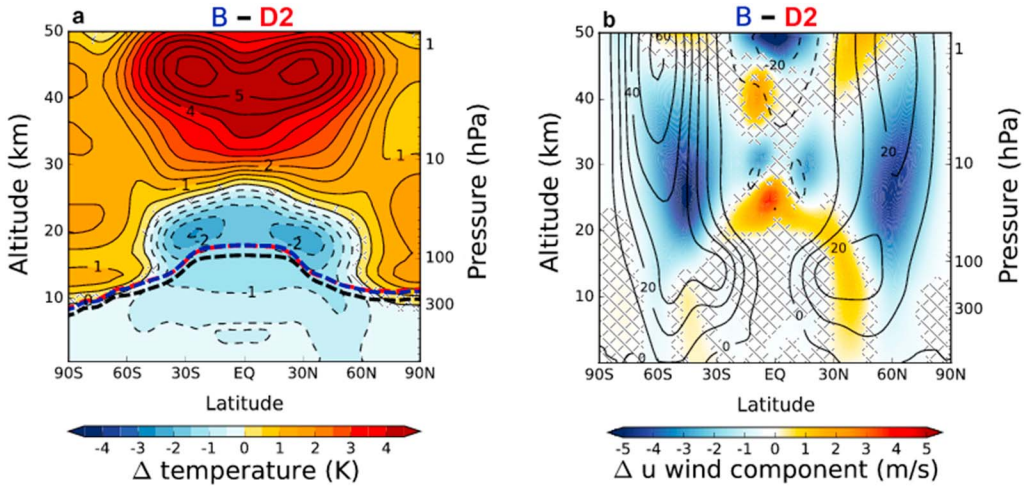

Figure 4. (a and b) Zonal mean temperature and zonal wind differences, as labeled, for years 50–200 after the 4xCO_2 forcing. In (a), the color scale is constrained to highlight the changes around the tropical tropopause, while the contour lines show the full extent of all changes as 0.5 K intervals. The thick dashed lines show the average height of the thermal tropopause for A (black), B (blue), and D2 (red), which is calculated based on the WMO lapse rate definition (WMO, 1957). In (b), contours show the climatology of run B.

high altitudes allow less radiation to propagate to lower levels of the atmosphere, thus reducing ozone production there. Finally, while less important for the climate sensitivity response discussed here, we also find significant differences in the lower stratospheric high-latitude response of ozone in D2 compared to B (Figures 3a–3c). The smaller ozone mass mixing ratios found in D2 (and D1) are likely due to the lower ozone concentrations in air transported downward from the upper stratosphere into this region as part of the upper branch of the Brewer-Dobson circulation (Butchart, 2014; Plumb, 2002).

Ozone is a key radiative heating agent in the tropical UTLS (Fueglistaler et al., 2009). Therefore, the decreases in ozone have a pronounced cooling effect there, which accordingly is smaller in D1/D2 than in B (Figures 3c and 4a). This has two important consequences, which mainly explain the less negative $\alpha_{CS\text{-}LW}$ parameters in D1/D2:

1. Ozone is a particularly effective greenhouse gas in the tropical UTLS (Hansen et al., 1997; Lacis et al., 1990; Stuber et al., 2005). Therefore, the smaller circulation-driven decreases in tropical UTLS ozone in D1/D2 will contribute to the CS-LW differences, compared to B.
2. Higher tropical UTLS temperatures increase the entry rates of water vapor into the stratosphere (Dessler et al., 2013; Fueglistaler et al., 2005), resulting in higher SVW concentrations in D1/D2 than in B (Figure 3d). Since SVW is a greenhouse gas, this amplifies the greenhouse warming effect of the positive ozone anomaly in D1/D2 relative to B (Stuber et al., 2001). SVW mixing ratios increased by an additional 1.5–2 ppmv in D1/D2 compared to B (absolute increases under 4xCO_2 are ~1–1.5 ppmv in B and ~3 ppmv in D1/D2; in fact, the latter results closely match the HadGEM2-ES results in CMIP5).

Following our argument in Nowack et al. (2015), we thus conclude that both changes in tropical UTLS ozone and the associated SVW feedback are the key drivers behind the less negative $\alpha_{CS\text{-}LW}$ parameters (and thus global warming) in D1/D2 than in B.

In D1/D2 the resulting meridional temperature gradient is smaller than in B (Figure 4a). As expected, we find the corresponding weakening of the annual mean midlatitude stratospheric jet in B (Figure 4b). Within the troposphere, the Hadley cell contracts in B (relative to D2), with stronger zonal winds equatorward, but weaker poleward. This ozone-change-induced dynamical response opposes the response to increased CO_2. Chiodo and Polvani (2016a) discussed a similar phenomenon in the Southern Hemisphere in their sensitivity study, although a direct comparison is difficult, due to slightly different experimental design.

We can also link the feedback differences in the CRE-LW component to a previously described mechanism (see Nowack et al., 2015, for details). The temperature effect (Figure 4a) of the underestimated tropical UTLS ozone changes in D1/D2 relative to B leads to reduced formation of upper tropospheric cirrus clouds (Figure 5), which trap LW radiation in the atmosphere (Kuebbeler et al., 2012; Nowack, 2015; Zelinka et al., 2013).

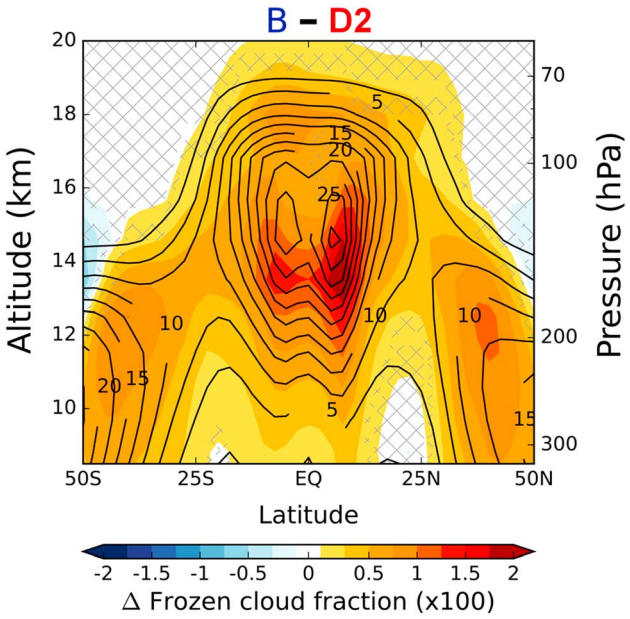

Figure 5. Differences in ice clouds, as labeled, for years 50–200 after the 4xCO_2 forcing. Nonsignificant changes at the 95% confidence level using a two-tailed Student's *t* test are hatched out. The contour lines show the climatology of simulation B.

Consequently, we find more negative $\alpha_{CRE\text{-}LW}$ parameters in D1/D2 than in B, which reduces the global warming gap between the simulations. In terms of absolute magnitude, this compensating effect almost cancels the CS-LW feedback differences, which gives rise to a much smaller discrepancy in the total feedback parameter α than if the model is run using fixed ozone throughout the entire atmosphere (Nowack et al., 2015). However, percentage-wise, the difference remains almost the same, with the CRE-LW effect being ~60% (70%) of the CS-LW effect for fixed ozone (D1/D2).

Finally, the more positive effective forcing F (larger by ~0.2 W/m^2 in the linear approximation) in D1/D2 than in B will contribute to the global warming differences; however, it is mechanistically more difficult to assign. It is the net result of differences in each of the four radiative components (see *y*-intercepts in Figures 2b–2e) that are too small to link to specific processes in a statistically robust manner. However, it is intuitive that fast ozone (and corresponding water vapor and temperature) changes have potential to affect the CS forcings, whereas their impact on absolute temperatures and lapse rates could indirectly affect the CRE forcings. We note that upper stratospheric ozone increases such as the ones suppressed in D1/D2 have mostly been associated with negative SW radiative forcing in studies with idealized ozone perturbations (e.g., Hansen et al., 1997; Lacis et al., 1990). We find no clear effect of ignoring upper stratospheric ozone changes on the CS-SW effective forcing (Figure 2d), which might simply be the result of its relatively small magnitude as compared to the tropical UTLS LW feedback associated with ozone, in agreement with the SW effects found in other studies (Dietmüller et al., 2014; Marsh et al., 2016). The reverse self-healing effect of the ozone column, which was not considered in the idealized perturbation studies, is presumably one reason for the small magnitude. The corresponding opposite sign upper and lower stratospheric changes in ozone are intrinsically coupled and have compensating SW effects.

4. Summary and Conclusions

We have discussed the impact of a specific climate model representation of ozone on the outcome of a standard climate sensitivity simulation. In this representation, ozone changes are only considered in the troposphere and the lowermost three model levels of the stratosphere. Comparing the model response to results obtained when including a fully interactive atmospheric chemistry scheme, we find a larger global warming resulting from (widely even more significant) regional surface temperature changes. These effects are mainly driven by the greenhouse effect of changes in tropical UTLS ozone and the related SVW feedback, which, however, is largely balanced by the radiative impact of simultaneous upper tropospheric cirrus cloud changes. We further find that fast adjustments (Sherwood et al., 2015; Zelinka et al., 2013) as a sum over all radiative components (clouds, clear-sky longwave, and shortwave) make a contribution to the larger global warming response. However, these are difficult to assign mechanistically in a statistically significant manner.

Our study has several implications. First, we identify a need to check influences of ozone's representation in climate sensitivity simulations, which are often poorly documented. One example for a noninteractive but somewhat adaptive ozone representation in a climate sensitivity simulation was given by Li et al. (2013). Using the climate model ECHAM5, they found a very large equilibrium surface warming effect of neglecting ozone changes. They thus decided to shift ozone from the highly sensitive upper troposphere into the upper stratosphere during the simulation, arguing that high levels of stratospheric ozone would otherwise continuously be shifted into the troposphere under CO_2-forced tropospheric expansion. Such physically inconsistent methods will become redundant as more sophisticated atmospheric chemistry components play a key role in the ever increasing complexity of climate models. However, we hope that our study will help to understand

past model results better and to motivate further studies in this direction. Ultimately, this could be helpful in tracking progress in climate modeling. For instance, using the same ozone representation, we find SVW increases very similar to those obtained with the predecessor model HadGEM2-ES in CMIP5. Our results thus imply that the use of a fully interactive chemistry scheme could have at least halved the SVW increase found then (from ~3 to ~1.5 ppmv), which is important for global energy budget considerations as well as atmospheric chemistry (Shindell, 2001; Stenke & Grewe, 2005; Stenke et al., 2008, 2009; Solomon et al., 2010). In addition, our study could motivate further research into how model representations of ozone affect regional climate change projections (Marvel, Schmidt, Miller, et al., 2015; Marvel, Schmidt, Shindell, et al., 2015; Shindell, 2014; Shindell et al., 2015) and key modes of climate variability such as the El Niño–Southern Oscillation (Chiodo & Polvani, 2016a; Nowack et al., 2017) rather than just global mean surface temperature change. Finally, our results also bear implications for the efficacy of ozone forcings considering simultaneous cloud feedbacks (Hansen et al., 1997, 2005; Stuber et al., 2005).

In conclusion, we highlight the need to better understand the effects of various model representations of ozone on surface climate change projections, in particular with regard to their impact on results of typical climate sensitivity simulations and the corresponding model-dependency. Among current estimates, the model used here lies at the upper end when it comes to the climate sensitivity impact of neglecting ozone feedback entirely, even if the sign of the response and mechanisms found across most models are robust (Dietmüller et al., 2014; Muthers et al., 2014; Nowack et al., 2015). Another model showed hardly any net effect on surface temperature (Marsh et al., 2016). The relatively large sensitivity of our model might imply also a relatively larger effect of the tropopause-height matching implementation on the modeled global warming. However, as implied by Figure 1, even relatively small global mean effects, such as the one found here (6–7%), can correspond to highly significant regional surface temperature changes. We therefore hope that future studies will provide a more complete picture of the impacts of ozone representations on global and regional climate sensitivity estimates.

Acknowledgments
We thank the European Research Council for funding through the ACCI project (project number 267760). The model development was part of the QESM-ESM project supported by the UK Natural Environment Research Council (NERC) under contract numbers RH/H10/19 and R8/H12/124. P. J. N. is supported through an Imperial College Research Fellowship. We acknowledge use of the MONSooN system, a collaborative facility supplied under the Joint Weather and Climate Research Programme, which is a strategic partnership between the UK Met Office and NERC. We used the JASMIN postprocessing system (Lawrence et al., 2013) provided through the Centre for Environmental Data Analysis (CEDA). For their roles in producing, coordinating, and making available the HadGEM2-ES CMIP5 model output, we acknowledge the UK Met Office, the World Climate Research Programme's (WCRP) Working Group on Coupled Modeling (WGCM), and the Global Organization for Earth System Science Portals (GO-ESSP). Study-specific data are available through the first author or CEDA (url: http://catalogue.ceda.ac.uk/uuid/3d23afc9bb024c558058749faae4cf2d).

References

Andrews, T., Gregory, J. M., Webb, M. J., & Taylor, K. E. (2012). Forcing, feedbacks and climate sensitivity in CMIP5 coupled atmosphere-ocean climate models. *Geophysical Research Letters*, *39*, L09712. https://doi.org/10.1029/2012GL051607

Bian, H., & Prather, M. J. (2002). Fast-J2: Accurate simulation of stratospheric photolysis in global chemical models. *Journal of Atmospheric Chemistry*, *41*(3), 281–296. https://doi.org/10.1023/A:1014980619462

Boer, G. J., & Yu, B. (2003a). Climate sensitivity and response. *Climate Dynamics*, *20*(4), 415–429. https://doi.org/10.1007/s00382-002-0283-3

Boer, G. J., & Yu, B. (2003b). Dynamical aspects of climate sensitivity. *Geophysical Research Letters*, *30*(3), 1135. https://doi.org/10.1029/2002GL016549

Butchart, N. (2014). The Brewer-Dobson circulation. *Reviews of Geophysics*, *52*, 157–184. https://doi.org/10.1002/2013RG000448.One

Chiodo, G., & Polvani, L. M. (2016a). Reduced Southern Hemispheric circulation response to quadrupled CO_2 due to stratospheric ozone feedback. *Geophysical Research Letters*, *44*, 465–474. https://doi.org/10.1002/2016GL071011

Chiodo, G., & Polvani, L. M. (2016b). Reduction of climate sensitivity to solar forcing due to stratospheric ozone feedback. *Journal of Climate*, *29*(12), 4651–4663. https://doi.org/10.1175/JCLI-D-15-0721.1

Cionni, I., Eyring, V., Lamarque, J. F., Randel, W. J., Stevenson, D. S., Wu, F., et al. (2011). Ozone database in support of CMIP5 simulations: Results and corresponding radiative forcing. *Atmospheric Chemistry and Physics*, *11*(21), 11,267–11,292. https://doi.org/10.5194/acp-11-11267-2011

Collins, W. J., Bellouin, N., Doutriaux-Boucher, M., Gedney, N., Halloran, P., Hinton, T., et al. (2011). Development and evaluation of an Earth-system model—HadGEM2. *Geoscientific Model Development*, *4*(4), 1051–1075. https://doi.org/10.5194/gmd-4-1051-2011

Dessler, A. E., Schoeberl, M. R., Wang, T., Davis, S. M., & Rosenlof, K. H. (2013). Stratospheric water vapor feedback. *Proceedings of the National Academy of Sciences of the United States of America*, *110*(45), 18,087–18,091. https://doi.org/10.1073/pnas.1310344110

Dietmüller, S., Ponater, M., & Sausen, R. (2014). Interactive ozone induces a negative feedback in CO2-driven climate change simulations. *Journal of Geophysical Research: Atmospheres*, *119*, 1796–1805. https://doi.org/10.1002/2013JD020575

Eyring, V., Arblaster, J. M., Cionni, I., Sedláček, J., Perlwitz, J., Young, P. J., et al. (2013). Long-term ozone changes and associated climate impacts in CMIP5 simulations. *Journal of Geophysical Research: Atmospheres*, *118*, 5029–5060. https://doi.org/10.1002/jgrd.50316

Eyring, V., Bony, S., Meehl, G. A., Senior, C. A., Stevens, B., Stouffer, R. J., & Taylor, K. E. (2016). Overview of the Coupled Model Intercomparison Project Phase 6 (CMIP6) experimental design and organization. *Geoscientific Model Development*, *9*(5), 1937–1958. https://doi.org/10.5194/gmd-9-1937-2016

Forster, P. M., Andrews, T., Good, P., Gregory, J. M., Jackson, L. S., & Zelinka, M. (2013). Evaluating adjusted forcing and model spread for historical and future scenarios in the CMIP5 generation of climate models. *Journal of Geophysical Research: Atmospheres*, *118*, 1139–1150. https://doi.org/10.1002/jgrd.50174

Forster, P. M., Richardson, T., Maycock, A. C., Smith, C. J., Samset, B. H., Myhre, G., et al. (2016). Recommendations for diagnosing effective radiative forcing from climate models for CMIP6. *Journal of Geophysical Research: Atmospheres*, *121*, 12,460–12,475. https://doi.org/10.1002/2016JD025320

Forster, P. M. D. E., & Shine, K. P. (1997). Radiative forcing and temperature trends from stratospheric ozone changes. *Journal of Geophysical Research*, *102*, 10,841–10,855. https://doi.org/10.1029/96JD03510

Fueglistaler, S., Bonazzola, M., Haynes, P. H., & Peter, T. (2005). Stratospheric water vapor predicted from the Lagrangian temperature history of air entering the stratosphere in the tropics. *Journal of Geophysical Research: Atmospheres*, *110*, D08107. https://doi.org/10.1029/2004JD005516

Fueglistaler, S., Dessler, A. E., Dunkerton, T. J., Folkins, I., Fu, Q., & Mote, P. W. (2009). Tropical tropopause layer. *Reviews of Geophysics*, *47*, RG1004. https://doi.org/10.1029/2008RG000267

Gabriel, A., Peters, D., Kirchner, I., & Graf, H. F. (2007). Effect of zonally asymmetric ozone on stratospheric temperature and planetary wave propagation. *Geophysical Research Letters*, *34*, L06807. https://doi.org/10.1029/2006GL028998

Gregory, J. M., Ingram, W. J., Palmer, M. A., Jones, G. S., Stott, P. A., Thorpe, R. B., et al. (2004). A new method for diagnosing radiative forcing and climate sensitivity. *Geophysical Research Letters*, *31*, L03205. https://doi.org/10.1029/2003GL018747

Gregory, J. M., & Webb, M. (2008). Tropospheric adjustment induces a cloud component in CO_2 forcing. *Journal of Climate*, *21*(1), 58–71. https://doi.org/10.1175/2007JCLI1834.1

Haigh, J. D., & Pyle, J. A. (1982). Ozone perturbation experiments in a two-dimensional circulation model. *Quarterly Journal of the Royal Meteorological Society*, *108*(457), 551–574. https://doi.org/10.1002/qj.49710845705

Hansen, J., Sato, M., & Ruedy, R. (1997). Radiative forcing and climate response. *Journal of Geophysical Research*, *102*, 6831–6864. https://doi.org/10.1029/96JD03436

Hansen, J., Sato, M., Ruedy, R., Nazarenko, L., Lacis, A., Schmidt, G. A., et al. (2005). Efficacy of climate forcings. *Journal of Geophysical Research*, *110*, D18104. https://doi.org/10.1029/2005JD005776

Heinemann, M. (2009). Warm and sensitive Paleocene-Eocene climate, Max Planck Institute for Meteorology, Hamburg, Germany.

Hewitt, H. T., Copsey, D., Culverwell, I. D., Harris, C. M., Hill, R. S. R., Keen, A. B., et al. (2011). Design and implementation of the infrastructure of HadGEM3: The next-generation Met Office climate modelling system. *Geoscientific Model Development*, *4*(2), 223–253. https://doi.org/10.5194/gmd-4-223-2011

Hoerling, M. P., Schaack, T. K., & Lenzen, A. J. (1993). A global analysis of stratospheric-tropospheric exchange during northern winter. *Monthly Weather Review*, *121*(1), 162–172. https://doi.org/10.1175/1520-0493(1993)121%3C0162:AGAOSE%3E2.0.CO;2

Hunke, E. C., & Lipscomb, W. H. (2008). the Los Alamos sea ice model documentation and software user's manual, Version 4.0, LA-CC-06-012, Los Alamos National Laboratory, N.M.

Jones, C. D., Hughes, J. K., Bellouin, N., Hardiman, S. C., Jones, G. S., Knight, J., et al. (2011). The HadGEM2-ES implementation of CMIP5 centennial simulations. *Geoscientific Model Development*, *4*(1), 689–763. https://doi.org/10.5194/gmdd-4-689-2011

Jonsson, A. I., de Grandpré, J., Fomichev, V. I., McConnell, J. C., & Beagley, S. R. (2004). Doubled CO_2-induced cooling in the middle atmosphere: Photochemical analysis of the ozone radiative feedback. *Journal of Geophysical Research*, *109*, D24103. https://doi.org/10.1029/2004JD005093

Knutti, R., & Rugenstein, M. A. A. (2015). Feedbacks, climate sensitivity and the limits of linear models. *Philosophical Transactions of the Royal Society A*, *373*(2054). https://doi.org/10.1098/rsta.2015.0146

Kravitz, B., Robock, A., Forster, P. M., Haywood, J. M., Lawrence, M. G., & Schmidt, H. (2013). An overview of the Geoengineering Model Intercomparison Project (GeoMIP). *Journal of Geophysical Research: Atmospheres*, *118*, 13,103–13,107. https://doi.org/10.1002/2013JD020569

Kuebbeler, M., Lohmann, U., & Feichter, J. (2012). Effects of stratospheric sulfate aerosol geo-engineering on cirrus clouds. *Geophysical Research Letters*, *39*, L23803. https://doi.org/10.1029/2012GL053797

Lacis, A. A., Wuebbles, D. J., & Logan, J. A. (1990). Radiative forcing of climate by changes in the vertical distribution of ozone. *Journal of Geophysical Research*, *95*, 9971–9981. https://doi.org/10.1029/JD095iD07p09971

Lawrence, B. N., Bennett, V. L., Churchill, J., Juckes, M., Kershaw, P., Pascoe, S., et al. (2013). Storing and manipulating environmental big data with JASMIN, *Proc. - 2013 IEEE Int. Conf. Big Data*, Big Data 2013, 68–75. https://doi.org/10.1109/BigData.2013.6691556

Li, C., von Storch, J.-S., & Marotzke, J. (2013). Deep-ocean heat uptake and equilibrium climate response. *Climate Dynamics*, *40*(5–6), 1071–1086. https://doi.org/10.1007/s00382-012-1350-z

Lin, P., & Fu, Q. (2013). Changes in various branches of the Brewer-Dobson circulation from an ensemble of chemistry climate models. *Journal of Geophysical Research: Atmospheres*, *118*, 73–84. https://doi.org/10.1029/2012JD018813

Madec, G. (2008). NEMO ocean engine, Note du Pole de modelisation, Institut Pierre-Simon Laplace (IPSL), 27th ed., France.

Marsh, D. R., Conley, A. J., & Polvani, L. M. (2016). Stratospheric ozone chemistry feedbacks are not critical for the determination of climate sensitivity in CESM1 (WACCM). *Geophysical Research Letters*, *43*, 3928–3934. https://doi.org/10.1002/2016GL068344

Marvel, K., Schmidt, G. A., Miller, R. L., & Nazarenko, L. S. (2015). Implications for climate sensitivity from the response to individual forcings. *Nature Climate Change*, *6*(4), 386–389. https://doi.org/10.1038/nclimate2888

Marvel, K., Schmidt, G. A., Shindell, D., Bonfils, C., LeGrande, A. N., Nazarenko, L., & Tsigaridis, K. (2015). Do responses to different anthropogenic forcings add linearly in climate models? *Environmental Research Letters*, *10*(10), 104010. https://doi.org/10.1088/1748-9326/10/10/104010

Meul, S., Langematz, U., Oberländer, S., Garny, H., & Jöckel, P. (2014). Chemical contribution to future tropical ozone change in the lower stratosphere. *Atmospheric Chemistry and Physics*, *14*(6), 2959–2971. https://doi.org/10.5194/acp-14-2959-2014

Morgenstern, O., Braesicke, P., O'Connor, F. M., Bushell, A. C., Johnson, C. E., Osprey, S. M., & Pyle, J. A. (2009). Evaluation of the new UKCA climate-composition model – Part 1: The stratosphere. *Geoscientific Model Development*, *2*(1), 43–57. https://doi.org/10.5194/gmd-2-43-2009

Muthers, S., Anet, J. G., Stenke, A., Raible, C. C., Rozanov, E., Brönnimann, S., et al. (2014). The coupled atmosphere–chemistry–ocean model SOCOL-MPIOM. *Geoscientific Model Development*, *7*(5), 2157–2179. https://doi.org/10.5194/gmd-7-2157-2014

Muthers, S., Raible, C. C., Rozanov, E., & Stocker, T. F. (2016). Response of the AMOC to reduced solar radiation—The modulating role of atmospheric chemistry. *Earth System Dynamics*, *7*(4), 877–892. https://doi.org/10.5194/esd-7-877-2016

Neu, J. L., Prather, M. J., & Penner, J. E. (2007). Global atmospheric chemistry: Integrating over fractional cloud cover. *Journal of Geophysical Research – Atmospheres*, *112*, D11306. https://doi.org/10.1029/2006JD008007

Noda, S., Kodera, K., Adachi, Y., Deushi, M., Kitoh, A., Mizuta, R., et al. (2017). Impact of interactive chemistry of stratospheric ozone on southern hemisphere paleoclimate simulation. *Journal of Geophysical Research: Atmospheres*, *122*, 878–895. https://doi.org/10.1002/2016JD025508

Nowack, P. J. (2015). Cirrus and the Earth system. *Weather*, *70*(11), 330. https://doi.org/10.1002/wea.2550

Nowack, P. J., Abraham, N. L., Braesicke, P., & Pyle, J. A. (2016). Stratospheric ozone changes under solar geoengineering: Implications for UV exposure and air quality. *Atmospheric Chemistry and Physics*, *15*(21), 31,973–32,004. https://doi.org/10.5194/acpd-15-31973-2015

Nowack, P. J., Braesicke, P., Abraham, N. L., & Pyle, J. A. (2017). On the role of ozone feedback in the ENSO amplitude response under global warming. *Geophysical Research Letters*, *44*, 3858–3866. https://doi.org/10.1002/2016GL072418

Nowack, P. J., Luke Abraham, N., Maycock, A. C., Braesicke, P., Gregory, J. M., Joshi, M. M., et al. (2015). A large ozone-circulation feedback and its implications for global warming assessments. *Nature Climate Change*, *5*(1), 41–45. https://doi.org/10.1038/nclimate2451

Plumb, R. A. (2002). Stratospheric transport. *Journal of the Meteorological Society of Japan*, *80*(4B), 793–809. https://doi.org/10.2151/jmsj.80.793

Price, C., & Rind, D. (1992). A simple lightning parameterization for calculating global lightning distributions. *Journal of Geophysical Research*, *97*, 9919–9933. https://doi.org/10.1029/92JD00719

Price, C., & Rind, D. (1994). Modeling global lightning distributions in a general circulation model. *Monthly Weather Review*, *122*(8), 1930–1939. https://doi.org/10.1175/1520-0493(1994)122%3C1930:MGLDIA%3E2.0.CO;2

Pyle, J. A. (1980). A calculation of the possible depletion of ozone by chlorofluorocarbons using a two-dimensional model. *Pure and Applied Geophysics*, *118*(1), 355–377. https://doi.org/10.1007/BF01586458

Riese, M., Ploeger, F., Rap, A., Vogel, B., Konopka, P., Dameris, M., & Forster, P. (2012). Impact of uncertainties in atmospheric mixing on simulated UTLS composition and related radiative effects. *Journal of Geophysical Research*, *117*, D16305. https://doi.org/10.1029/2012JD017751

Sherwood, S. C., Bony, S., Boucher, O., Bretherton, C., Forster, P. M., Gregory, J. M., & Stevens, B. (2015). Adjustments in the forcing-feedback framework for understanding climate change. *Bulletin of the American Meteorological Society*, *96*(2), 217–228. https://doi.org/10.1175/BAMS-D-13-00167.1

Shindell, D., & Faluvegi, G. (2009). Climate response to regional radiative forcing during the twentieth century. *Nature Geoscience*, *2*(4), 294–300. https://doi.org/10.1038/ngeo473

Shindell, D. T. (2001). Climate and ozone response to increased stratospheric water vapor. *Geophysical Research Letters*, *28*, 1551–1554. https://doi.org/10.1029/1999GL011197

Shindell, D. T. (2014). Inhomogeneous forcing and transient climate sensitivity. *Nature Climate Change*, *4*(4), 274–277. https://doi.org/10.1038/NCLIMATE2136

Shindell, D. T., Faluvegi, G., Rotstayn, L., & Milly, G. (2015). Spatial patterns of radiative forcing and surface temperature response. *Journal of Geophysical Research: Atmospheres*, *120*, 5385–5403. https://doi.org/10.1002/2014JD022752

Soden, B. J., Broccoli, A. J., & Hemler, R. S. (2004). On the use of cloud forcing to estimate cloud feedback. *Journal of Climate*, *17*(19), 3661–3665. https://doi.org/10.1175/1520-0442(2004)017%3C3661:OTUOCF%3E2.0.CO;2

Soden, B. J., Held, I. M., Colman, R. C., Shell, K. M., Kiehl, J. T., & Shields, C. A. (2008). Quantifying climate feedbacks using radiative kernels. *Journal of Climate*, *21*(14), 3504–3520. https://doi.org/10.1175/2007JCLI2110.1

Solomon, S., Rosenlof, K. H., Portmann, R. W., Daniel, J. S., Davis, S. M., Sanford, T. J., & Plattner, G.-K. (2010). Contributions of stratospheric water vapor to decadal changes in the rate of global warming. *Science*, *327*(5970), 1219–1223. https://doi.org/10.1126/science.1182488

Son, S.-W., Polvani, L. M., Waugh, D. W., Akiyoshi, H., Garcia, R., Kinnison, D., et al. (2008). The impact of stratospheric ozone recovery on the Southern Hemisphere westerly jet. *Science*, *320*(5882), 1486–1489. https://doi.org/10.1126/science.1155939

SPARC (2010). SPARC CCMVal report on the evaluation of chemistry-climate models. In V. Eyring, T. G. Shepherd, & D. W. Waugh (Eds.), SPARC report no. 5, WCRP-132, WMO/TD-No. 1526.

Stenke, A., Dameris, M., Grewe, V., & Garny, H. (2009). Implications of Lagrangian transport for simulations with a coupled chemistry-climate model. *Atmospheric Chemistry and Physics*, *9*(15), 5489–5504. https://doi.org/10.5194/acp-9-5489-2009

Stenke, A., & Grewe, V. (2005). Simulation of stratospheric water vapor trends: Impact on stratospheric ozone chemistry. *Atmospheric Chemistry and Physics*, *5*(5), 1257–1272. https://doi.org/10.5194/acp-5-1257-2005

Stenke, A., Grewe, V., & Ponater, M. (2008). Lagrangian transport of water vapor and cloud water in the ECHAM4 GCM and its impact on the cold bias. *Climate Dynamics*, *31*(5), 491–506. https://doi.org/10.1007/s00382-007-0347-5

Stuber, N., Ponater, M., & Sausen, R. (2001). Is the climate sensitivity to ozone perturbations enhanced by stratospheric water vapor feedback? *Geophysical Research Letters*, *28*, 2887–2890. https://doi.org/10.1029/2001GL013000

Stuber, N., Ponater, M., & Sausen, R. (2005). Why radiative forcing might fail as a predictor of climate change. *Climate Dynamics*, *24*(5), 497–510. https://doi.org/10.1007/s00382-004-0497-7

Taylor, K. E., Stouffer, R. J., & Meehl, G. A. (2012). An overview of CMIP5 and the experiment design. *Bulletin of the American Meteorological Society*, *93*(4), 485–498. https://doi.org/10.1175/BAMS-D-11-00094.1

Telford, P. J., Abraham, N. L., Archibald, A. T., Braesicke, P., Dalvi, M., Morgenstern, O., et al. (2013). Implementation of the Fast-JX Photolysis scheme (v6.4) into the UKCA component of the MetUM chemistry-climate model (v7.3). *Geoscientific Model Development*, *6*(1), 161–177. https://doi.org/10.5194/gmd-6-161-2013

Voulgarakis, A., & Shindell, D. T. (2010). Constraining the sensitivity of regional climate with the use of historical observations. *Journal of Climate*, *23*(22), 6068–6073. https://doi.org/10.1175/2010JCLI3623.1

Wild, O., Zhu, X., & Prather, M. J. (2000). Fast-J: Accurate simulation of in- and below-cloud photolysis in tropospheric chemical models. *Journal of Atmospheric Chemistry*, *37*(3), 245–282. https://doi.org/10.1023/A:1006415919030

WMO (1957). Meteorology—A three dimensional science: Second session of the Commission for Aerology, in *WMO Bull 4* (pp. 134–138).

Zelinka, M. D., Klein, S. A., Taylor, K. E., Andrews, T., Webb, M. J., Gregory, J. M., & Forster, P. M. (2013). Contributions of different cloud types to feedbacks and rapid adjustments in CMIP5. *Journal of Climate*, *26*(14), 5007–5027. https://doi.org/10.1175/JCLI-D-12-00555.1